

IMPACT OF TGF- β /SMAD SIGNALING AND OXIDATIVE STRESS IN RENAL FIBROSIS. IS THERE A LINK?

Hamada S. Qebes^{1*}, Mohamed A. Abdel Aziz¹, Ahmed A. Abdel Ghany¹,
Madiha M Zakhary², Abdel-Razik H. Abdel-Razik³

¹ Department of Biochemistry, Faculty of Pharmacy, Al-Azhar University, Assiut, Egypt.

² Department of Biochemistry, Faculty of Medicine, Assiut University, Assiut, Egypt.

³ Department of Histology, Faculty of Veterinary Medicine, Beni-Suef University, Beni-Suef, Egypt

*Corresponding author: E-mail: hamadaabozaid@azhar.edu.eg

ABSTRACT

Chronic kidney disease (CKD) has emerged as a major cause of morbidity and mortality worldwide. Irrespective of the cause, renal fibrosis is considered the common final pathway of all kidney diseases driving to end stage renal disease (ESRD). Although some previous studies focused on the involvement of both reactive oxygen species (ROS) and TGF- β /Smad signaling in the development of fibrosis, only few studies highlight on the potential relationship between them in renal fibrosis, so the current study aimed to explore the impact of both ROS and TGF- β /Smad signaling on renal fibrosis on the one hand and to clarify the relationship between them on the other hand, using a mice model of unilateral ureteral obstruction (UUO). Mice were randomized to (n=10/group): sham operated, 3 days ligated, 7 days ligated and 14 days ligated groups. The mice were sacrificed after 3, 7 and 14 days of ligation. Smad3, Smad4 and vimentin were investigated by western blotting while the mRNA level of TGF- β 1 was assessed by qRT-PCR. The renal tissue levels of malonaldehyde (MDA), nitric oxide (NO) and reduced glutathione (GSH) besides superoxide dismutase (SOD) activity were assayed calorimetrically. Our immunoblotting results revealed overexpression of Smad3, Smad4 and vimentin in the obstructed kidneys compared to the Sham-operated kidneys. QRT-PCR results, showed TGF- β 1 up-regulation coincided with significant disruptions in the oxidant/antioxidant system. In conclusion, our findings revealed that ROS can modulate TGF- β 1 signaling through different pathways including Smad pathway. On the other hand, TGF- β 1 could induce ROS production and inhibit antioxidant system, resulting in redox disturbance. These findings suggest an interesting cycle of TGF- β 1 and ROS interplay.

Keywords: Chronic kidney disease, Renal fibrosis, Unilateral ureteral obstruction, TGF- β 1, Smad3, Smad4, Vimentin, Reactive oxygen species

INTRODUCTION

Chronic kidney disease (CKD) has been recognized as an important public health issue around the world, with global assessed predominance of 13.4% (**Lv and Zhang, 2019**). Renal fibrosis, characterized by excessive deposition of Extracellular matrix (ECM), is considered a common pathological feature of CKD resulting in the development of End-stage renal disease (ESRD) (**Meng et al., 2015**). In such fibrotic processes, kidney fibroblasts play pivotal roles, however the origin of fibroblasts remain unclear (**El Agha et al., 2017; Di Carlo and Peduto, 2018**). Activated fibroblasts could secrete different types proteins such as procollagen, and proteoglycans which form a part of ECM (**Kendrick and Chonchol, 2011; Boor and Floege, 2012**). Myofibroblast is a special kind of fibroblasts that has developed some smooth muscle cells characteristics. It could express different mesenchymal cells markers including α -smooth muscle actin (α -SMA), collagen I, fibronectin and adhesion molecules. (**Boor and Floege, 2012**).

On the other hand, epithelial mesenchymal transition (EMT) is considered one of the most important mechanisms that implicated in the pathogenesis of renal fibrosis (**Liu, 2010**). EMT comprises a series of events through which epithelial cells lose their epithelial characteristics and gain new properties of typical mesenchymal cells (**Marquez-Exposito et al., 2018**).

As is true in other organs, fibrosis of the kidney can be induced by multiple stimuli or mediators via multiple mechanisms. Among them, transforming growth factor- β 1 (TGF- β 1) has served as an important and crucial mediator in the pathogenesis of renal fibrosis (**Duffield, 2014; Chen et al., 2017; Zhang et al., 2017**). It has been reported that, TGF- β 1 is involved in the fibrotic process via transformation of tubular epithelial cells into ECM producing fibroblasts or myofibroblasts. Moreover, It has the ability to induce EMT (**Chen et al., 2018**). TGF- β 1 can exert its biological functions through a variety of signaling pathways, including canonical (Smad-based) and non-canonical (non-Smad based) pathways (**Meng et al., 2015**).

Smads comprise a family of structurally related proteins containing two globular domains connected together by a linker region. These domains are called Mad homology 1 (MH1) at the N-terminus, and MH2 at the C-terminus. MH1 domain, is responsible for DNA binding, while the main function of MH2 domain, is to mediate protein-protein interaction with various regulators and effector proteins, including the TGF- β 1 receptor (TGF β RI) (**Macias et al., 2015**). Three classes of Smads including receptor- regulated Smads (R-Smads), common mediator Smads (Co- Smads) and inhibitory Smads (I-Smads) have been identified in biological system. The R-Smads including Smad1, Smad3, Smad5 and Smad8 are directly activated via phosphorylation by TGF β RI forming a heterooligomeric complex with the common mediator Smad4. This complex then shuttles into the nucleus where it is recruited into DNA by specific DNA-binding transcription factors and regulates transcription of target gene (**Budi et al., 2017; Lucarelli et al., 2018**).

Although the exact mechanism is not fully understood, some evidences indicated that oxidative stress plays a pivotal role in the pathogenesis of renal fibrosis.

Oxidative stress results from disturbance between the production of free radicals and reduced anti-oxidant defenses (Lv et al., 2018). Several studies have demonstrated that oxidative stress may occur secondary to activation of TGF- β 1 activity (Lee et al., 2015). In spite of other previous studies that demonstrated the role of both ROS and TGF- β 1/Smad signaling in the development of fibrosis, only few studies focused on the relationship between ROS and TGF- β 1. Based on that, the current study aimed to explore involvement of both ROS and TGF- β 1/Smad signaling in the development of renal fibrosis. Furthermore, our study aimed to clarify the potential relationship between TGF- β 1/Smad signaling pathway and oxidative stress in renal fibrosis, using a mice model of unilateral ureteral obstruction (UUO).

MATERIALS AND METHODS

Animals and experimental design

Animal experiments were performed after approval by the Institutional Animal Care and Use Committee of Faculty of Medicine, Assiut University, Assiut. 6 to 8-weeks-old male balb/c mice with body weight of 18–22 g, were purchased from the laboratory animal colony, Assiut University. Animals were allowed to acclimatize in the experimental laboratory for two weeks. Mice were housed (5 per cage) in wire-floored cages at a regulated environment (temperature, $22 \pm 2^\circ\text{C}$; humidity, $50 \pm 5\%$; night/day cycle, 12 hours) with free access to standard pellet diet and tap water *ad libitum*. Animal's weights were taken every other day and animal's behavior was monitored daily.

Unilateral ureteral obstruction (UUO) Model

Subsequent to acclimatization of the animals, the UUO model was performed under intraperitoneally anesthesia with an anesthetic solution of 100 mg/kg ketamine and 10 mg/kg xylazine. Following flank incision, left ureter was exposed. UUO was performed aseptically by complete ligation of the left ureter with 5-0 silk at two sites between the bladder and renal pelvis. (Chevalier et al., 2009). The mice were observed closely after surgery. Food and water intake and body weight were also monitored. Forty Mice were randomly assigned into 4 groups as follow: 3 days ligated group (n=10), 7 days ligated group (n=10), 14 days ligated group (n=10) and Sham-operated group (n=10), will receive the same surgical procedures but without ureter ligation.

One day before the experiment termination of each group, each animal was kept in an individual metabolic cage for 24 hours urine collection. The collected urine samples were centrifuged to remove cells and particulate material and then stored at -20°C for subsequent evaluation of the urinary biochemical parameters. One day later, blood samples were collected from retro-orbital plexus for serum preparation and the animals were sacrificed by cervical decapitation. The left kidney of each animal was excised, purified from adhering fat and connective tissues and washed in ice-cold isotonic saline. The excised kidney then divided into 3 parts; one part was stored in 10% neutral buffered formalin solution and subjected for histopathological examination. The other two parts were kept in RNA later solution and stored separately at -80°C for subsequent biochemical and molecular assays.

Histopathological assessment of kidney tissues

For histopathological examination, kidney tissues were fixed in 10% neutral buffered formalin solution for two days, dehydrated in ascending grades of ethanol, cleared in xylene, embedded in paraffin and sectioned at a thickness of 4–5 μm . Sections were stained with hematoxylin and eosin (H&E) and masson trichrome (MTC) according to previously described method (Suvarna et al., 2018). The section fields were examined under a light microscope (Olympus, USA) by a specialized histopathologist who was blinded to the groups' arrangement. The histopathological changes were scored according to previously described method (Gibson-Corley et al., 2013) as follows: normal appearance (0), 25% change (1), 26–50% change (2), 51–75% change (3), and 76–100% change (4) as mentioned in Table 1.

Table 1: Histopathological lesions score (H&E).

Histopathological lesions	Grou p 1	Grou p 2	Grou p 3	Grou p 4
Degenerated renal tubules/field	0	1	2	3
Degenerated renal corpuscle/field	0	1	1	2
Cystic dilatation of the renal tubules/field	0	1	2	1
Congestion	0	1	2	3
Cast	0	1	2	1
Interstitial inflammation	0	1	3	4

Group 1: sham; Group 2: UUO 3- days; Group 3: UUO 7- days; Group 4: UUO 14- days. (0) no change; (1) 25% change; (2) 26–50% change; (3) 51–75% change; (4) 76–100% change.

Assessment of biochemical indices of renal function

Serum creatinine (SCr) was assayed by kinetic procedure using a kit provided from Human Diagnostic (Wiesbaden, Germany). Blood urea nitrogen (BUN) was assayed by colorimetric procedure using a kit provided from Biomerieux Sa (Lyon, France). Microalbuminuria was estimated by colorimetric procedure using a kit provided from BioSystems (Barcelona, Spain).

Assessment of tissue levels of oxidant/antioxidant markers

Malonaldehyde (MDA), a lipid hydroperoxide, is formed by β -scission of peroxidized polyunsaturated fatty acids and is commonly measured by derivatization with thiobarbituric acid (TBA) to yield a red compound. MDA was determined spectrophotometrically in renal tissue homogenates at 535 and 520 nm in the form of thiobarbituric acid reacting substance (TBARS) and is expressed as equivalents of MDA, using 1, 1, 3, 3 tetramethoxypropane as standard (Mihara and Uchiyama, 1978). Results were expressed as $\mu\text{mol/g}$ protein. Based on the Griess reaction, nitric oxide (NO) was assayed spectrophotometrically in the renal tissue homogenates in the form of its stable metabolites particularly, nitrite (NO_2) and nitrate (NO_3) (Sessa et al., 1994). Results were expressed as $\mu\text{mol/mg}$ protein.

Reduced glutathione (GSH) was assayed spectrophotometrically in the renal tissue homogenates at 412 nm using Ellman assay method (Ellman, 1959). Results were expressed as $\mu\text{mol}/\text{mg}$ protein. Superoxide dismutase (SOD) activity in the renal tissue homogenates was assayed using kinetic procedures that based on the ability of SOD to inhibit the autooxidation of pyrogallol at alkaline medium (pH 8.2) (Mathupala et al., 1997). The enzymatic activity is expressed as U/mg protein. One unit is equivalent to the amount of SOD required to inhibit 50% of pyrogallol autooxidation.

Western blotting analysis

Kidney tissues were homogenized in Tris-HCL lysis buffer (400mM NaCl, 0.5% Triton X-100, 50mM Tris-HCL pH 7.4), incorporating 1% protease inhibitor cocktail (cell signaling technology, Inc, MA, USA) with the aid of Potter-Elvehjem rotor-stator homogenizer, fitted with a Teflon Pestle (Omni International, Kennesaw, GA, USA). Tissue residual was removed by centrifugation at $12000\times g$ for 10 min at 4 °C. Concentrations of total protein were measured by Biuret method (Wang et al., 1996). Equal amounts of protein (50 μg of total protein in each lane) were resolved by 12.5% SDS-polyacrylamide gel electrophoresis and transferred to a PVDF membrane using T-77 ECL semidry transfer unit (Amersham Biosciences UK Ltd) for 2 hours. The membrane was blocked with 5% non-fat milk in TBST buffer at room temperature for 1 hour and then incubated overnight with primary antibody at 4 °C. The antibodies used were anti-Smad3, Smad4 and vimentin antibodies (Santa Cruz, Dallas, USA dilution 1:1000) and anti- β -actin antibody (Thermo Fisher Scientific, USA, dilution 1:1000). The membrane was then incubated for 1 hour with an alkaline phosphatase-conjugated goat anti-mouse secondary antibody (Novus Biologicals, LLC, Littleton, CO, USA, dilution 1:5000). Bands were visualized by BCIP/NBT substrate detection Kit (Genemed Biotechnologies, Inc., CA, USA). All experiments were repeated to assure reproducibility of the results. The western blot analysis of β -actin was performed as an internal control of protein loading and the density of each band is determined using a digital imaging software program (Image J® software, National Institutes of Health, Bethesda, USA) and expressed as % of β -actin density.

Quantitative real-time PCR (qRT-PCR)

Total cellular RNA of kidney tissues was extracted using the Qiagen RNeasy Kit, according to the manufacturer's instructions. Eluted RNA was quantified using a Nano Drop (ND1000 spectrophotometer). cDNA was reverse transcribed from total RNA using qScript™ reverse transcriptase kit (Quanta Bioscience, cat no. 95048-500) according to the manufacturer's instructions and stored at -80 °C for subsequent experiments. QRT-PCR was performed using StepOnePlus with SYBR Green. mRNA level was normalized to GAPDH which produced comparable results. qRT-PCR reaction conditions comprised initial denaturation at 95 °C for 10 min, followed by 40 cycles of 95 °C for 15 seconds and 60 °C for 60 seconds. A melt curve analysis was performed at the end of each run of the SYBR Green protocol to confirm the generation of specific PCR products. The fold change of each gene was calculated using the delta-delta threshold ($\Delta\Delta\text{Ct}$) data analysis method.

Table 2: primers sequence used for QRT-PCR.

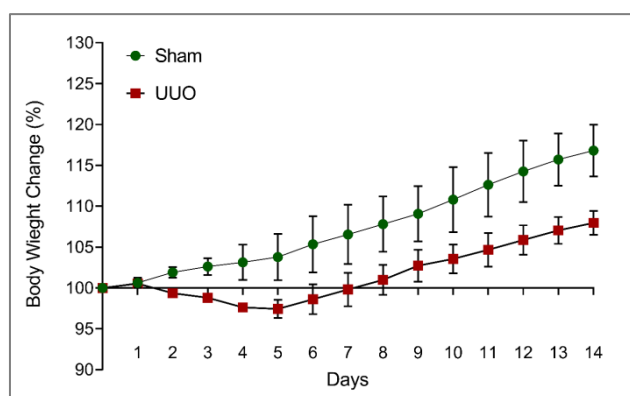
Targeted gen	sequence
TGF- β 1	F: 5- TGGAGCAACATGTGGA ACTC -3 R: 5- GTCAGCAGCCGGTTACCA -3
GAPDH	F: 5- GGGTTCCTATAAATACGGACTGC -3 R: 5- CCATTTTGTCTACGGGACGA -3

Statistical analysis

Statistical analyses of the obtained data were carried out using GraphPad prism version 8.0 (Graph pad software San Diego, USA). Data comparisons were performed using analysis of variance (ANOVA) followed by Tukey's t-test. The levels of significance were accepted with $p < 0.05$ and all relevant results were graphically displayed as mean \pm SEM.

RESULTS**Effect of UUO on body weight and mortality rate of mice along the experiment**

As illustrated in Fig. 1, all animals in the Sham-operated group gained significant body weight as compared to their corresponding initial body weight. Mice with UUO showed a temporary decrease in body weight. However shortly after that, they started to regain weight again with smaller rate compared to sham group (Figure 1). On the other hand, all animals remained alive throughout the experimental period except for a single mortality which was recorded on day 8 of the UUO 14- days group.

**Figure 1:** Effect of UUO on body weight of mice along the experiment**Histopathological changes in the kidneys of UUO mice**

H&E staining of kidneys obtained from sham-operated and UUO mice are shown in Figure (2-B). In the UUO 3-days group, the glomerular morphology was almost normal compared with the Sham-operated group, whereas the tubules were expanded with mildly broadened interstitial space and inflammatory cell infiltration in the interstitium with few corpuscles suffered from degeneration (G1). The renal tubules showed cystic dilatation. In the UUO 7-days and 14-days groups, most of the

Bowman’s capsules were broadened, several of the glomeruli were destroyed, several tubules displayed atrophy with a thickened basement membrane, and the interstitium was notably broader and displayed significant inflammatory cell infiltration in the interstitial space. Renal corpuscles suffered from degeneration, the renal tubules showed cystic dilatation and containing acidophilic materials (arrow) with congestion of the renal blood vessels (V), enclosed by lymphocytic infiltration (L).

MTC staining (2-C) revealed increased collagen fiber condensation between renal tubules in UUO mice in a time-dependent manner as compared to the Sham-operated mice which showed only fine collagenic fibers between the renal tubules and around the blood vessels. Massive condensation of collagen fiber was observed in UUO-14 days group indicating an excessive fibrotic renal damage. All these changes in the renal tissue suggested that the UUO model was successful and that typical fibrosis appeared after UUO.

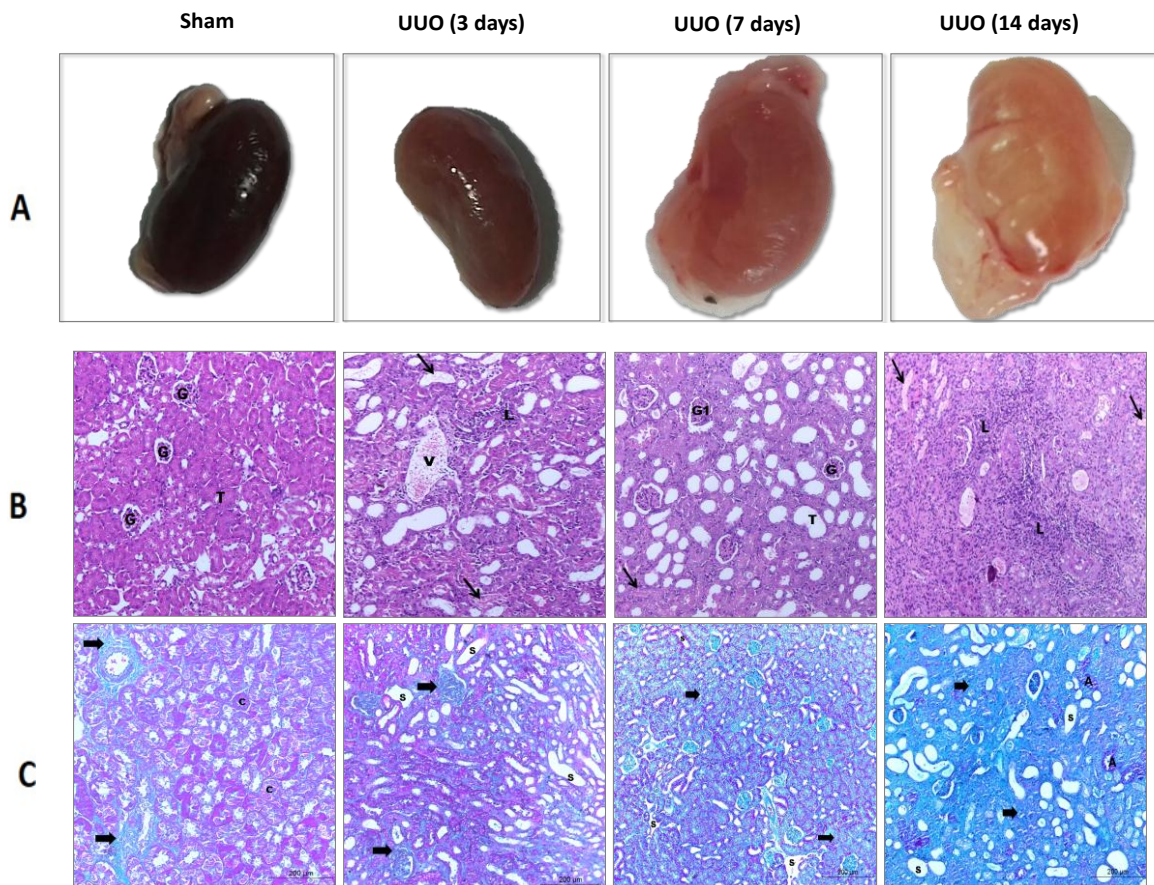


Figure 2: Morphological and histopathological changes in sham-operated and UUO mice. (A): Macroscopic findings of sham-operated and UUO groups. (B) Photomicrographs of kidney sections stained with H&E: kidney sections from Sham-operated group showed normal kidney histological structure. Kidney sections from UUO 14- days group showed tubular atrophy and dilation, infiltration of inflammatory cells, and interstitial fibrosis. These findings were less pronounced in UUO 3-days and UUO 7-days groups. (C): Photomicrographs of kidney sections stained with MTC: Sham-operated group showed normal collagen deposition. Kidney sections from UUO

14- days group showed collagenic fibers massively condensed between renal tubules. These findings were less pronounced in UUO 3-days and UUO 7-days groups.

Assessment of biochemical indices of renal function

As shown in table (3), the overall estimated biochemical indices of renal function matched their corresponding levels in the Sham-operated group without any observed significant differences in UUO 3- days and 7- days groups. In UUO 14- days group, SCr, BUN and microalbuminuria showed significant increase ($p<0.05$, $p<0.01$ and 0.05 respectively) as compared to the Sham-operated group.

Table 3: Changes in the biochemical indices of renal function including Scr, BUN and microalbuminuria.

	Sham	UUO 3- days	UUO 7- days	UUO 14- days
SCr(mg/dl)	0.36±0.011	0.38±0.01	0.40±0.016	0.42±0.013*
BUN(mg/dl)	15.93±0.84	17.37±0.95	19.55±1.006	22.30±1.12**.
Microalbuminuria (mg/l)	18.00±1.46	19.33±1.08	20.50±1.23	24.17±1.14*

Data are presented as mean ± SEM (n=6). *, • and ° indicate significant change from Sham, UUO 3- days and UUO 7- days, respectively. *, • and ° indicate significant change at $p<0.05$, **, **• and °° indicate significant change at $p<0.01$. ****, ****• and °°° indicate significant change at $p<0.001$. SCr, serum creatinine; BUN, blood urea nitrogen.

QRT-PCR assessment of the mRNA level of TGF-β1

As illustrated in Figure 3, our QRT-PCR results revealed upregulation of TGF-β1 mRNA expression after UUO in the obstructed kidney in comparison to the Sham-operated kidney. This upregulation in TGF-β1 mRNA expression was more evident at 14- UUO days (5 fold) than 7- UUO days (3.4 fold) which also was significant than 3- UUO days (1.7 fold) indicating a gradual increase in TGF-β1 mRNA expression among the different groups of UUO model (Figure 3).

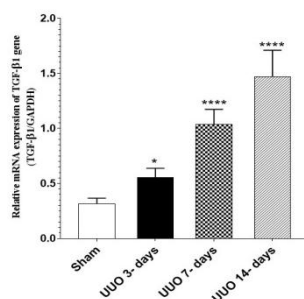


Figure 3: Representative analysis of mRNA expressions of TGF-β1 in renal tissue homogenates of sham-operated and UUO mice. mRNA expressions were measured by

quantitative RT-PCR analysis. Data are presented as mean \pm SEM (n = 6). * indicate significant change at $p < 0.05$; ** indicate significant change at $p < 0.01$; *** indicate significant change at $p < 0.001$.

Immunoblotting detection of Smad3, Smad4 and vimentin proteins

As illustrated in Figure 4A, Smad3 protein showed an over-expression in all groups of UUO model in comparison to the Sham-operated group with gradual increase from UUO 3- days group to reach its maximum at UUO 14- days group. (Figure 4A). Likewise, in comparison to the Sham-operated group, Smad4 protein showed apparent over-expression in fibrotic kidney tissues with UUO, especially at UUO 7-days and 14- days group (Figure 4B). Moreover, our immunoblotting data showed over expression of vimentin protein in in the obstructed kidney in comparison to the Sham-operated kidney. This over expression was more significant at UUO 7-days and 14- days' group when compared to UUO 3- days group (Figure 4C).

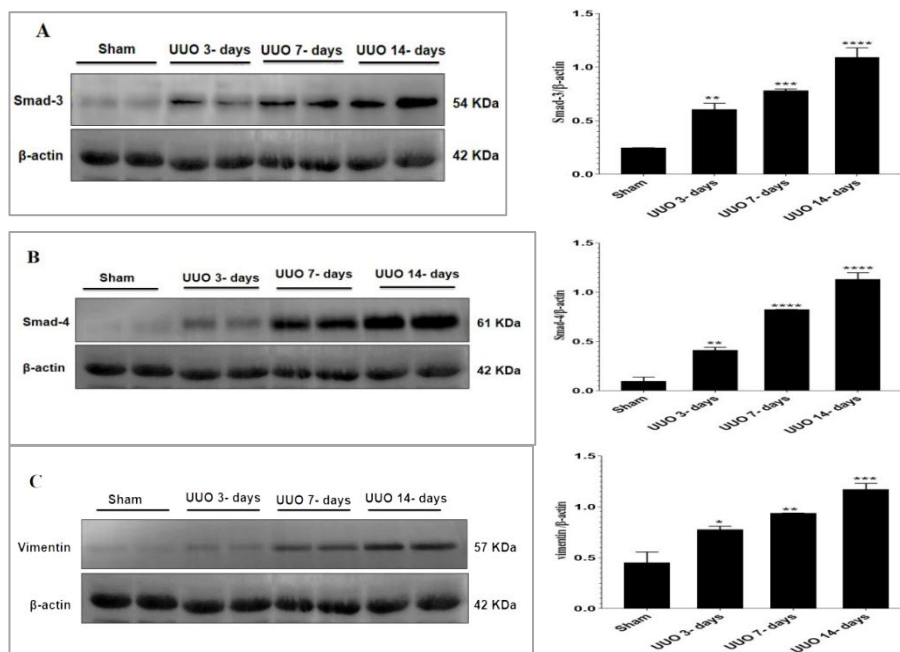


Figure 4: Representative Western blotting analysis of Smad3 (A), Smad4 (B) and vimentin (C) in renal tissue homogenates of Sham-operated and UUO mice. β -actin was used in parallel as an internal control. Data are presented as mean \pm SEM (n = 6). * indicate significant change at $p < 0.05$; ** indicate significant change at $p < 0.01$; *** indicate significant change at $p < 0.001$.

Assessment of oxidative stress markers

In comparison to the Sham-operated group, MDA and NO were significantly increased in 3- days UUO group ($p < 0.05$ and $p < 0.01$ respectively), 7- days UUO group ($p < 0.001$ and $p < 0.001$, respectively) and 14- days UUO group ($p < 0.001$ and $p < 0.001$, respectively). These increase in renal tissue contents of MDA and NO were significant in 7- days UUO ($p < 0.001$ and $p < 0.001$, respectively) and 14- days UUO ($p < 0.001$ and $p < 0.001$, respectively) groups when compared to 3- days UUO group. In 14- days UUO

group, renal tissue contents of MDA showed significant increase ($p < 0.01$) as compared to 7- days UO group, while there was no significant increase in renal tissue contents of NO in 14- days UO group as compared to 7- days UO group (Table 4).

On the other hand, GSH content and SOD activity were significantly reduced in the renal tissue homogenates of 7- days UO ($p < 0.05$ and $p < 0.01$, respectively), and 14- days UO ($p < 0.001$ and $p < 0.001$, respectively) groups in comparison to the Sham-operated group, while there was no significant difference in 3- days UO group as compared to the Sham-operated group (Table 4). When compared to 3- days UO group, the decrease in GSH content and SOD activity were significant in both 7- days UO group ($p < 0.05$ and $p < 0.01$, respectively) and 14- days UO group ($p < 0.001$ and $p < 0.001$, respectively). In comparison to 7- days UO group, there was significant decrease in GSH content in 14- days UO group ($p < 0.001$), but there was no significant decrease in SOD activity in the same group when compared to 7- days UO group.

Table 4: Levels of MDA, NO, GSH and SOD as markers of oxidative stress in sham and obstructed kidney tissue homogenates of different groups.

	Sham	UO 3- days	UO 7- days	UO 14- days
MDA($\mu\text{mol/g}$ protein)	31.17 \pm 0.52	35.07 \pm 1.18 [*]	42.07 \pm 0.66 ^{****,***}	47.48 \pm 0.88 ^{****,***,°°}
NO($\mu\text{mol/mg}$ protein)	55.98 \pm 1.65	62.81 \pm 1.15 ^{**}	82.92 \pm 1.29 ^{****,***}	87.25 \pm 1.21 ^{****,***}
GSH($\mu\text{mol/mg}$ protein)	82.00 \pm 1.04	79.37 \pm 1.35	67.83 \pm 4.39 ^{*,°}	46.98 \pm 3.258 ^{****,***,°°°}
SOD (U/mg protein)	15.48 \pm 0.42	14.92 \pm 0.31	12.05 \pm 0.44 ^{***,°°}	11.25 \pm 0.56 ^{****,***}

Data are presented as mean \pm SEM (n=6). *, ° and ° indicate significant change from Sham, UO 3- days and UO 7- days, respectively. *, ° and ° indicate significant change at $p < 0.05$, **, °° and °° indicate significant change at $p < 0.01$. ****, °°° and °°° indicate significant change at $p < 0.001$. MDA, malonaldehyde; NO, nitric oxide; SOD, superoxide dismutase; GSH, reduced glutathione.

DISCUSSION

Chronic kidney disease (CKD) represents a major healthcare burden and a dominant cause of death worldwide. Irrespective of the cause, renal fibrosis is the common final pathway of all kidney diseases driving to end stage renal disease (ESRD) (Meng et al., 2015). In Egypt, the assessed annual frequency of ESRD is around 74 per million and the overall predominance of patients on dialysis is 264 per million. The predominance rate of ESRD in Assiut governorate, was 366 per million and obscure etiology was the most common cause of ESRD (El-Arbagy et al., 2016).

Due to the different causes of renal failure, several animal models have been established to enhance our understanding of human nephropathy. Among them, rodents have been broadly utilized (Bao et al., 2018). In the current study, UO was utilized to imitate the development of obstructive nephropathy. Ureteral obstruction results in a

marked inflammatory and fibrotic response, followed by infiltration of inflammatory cells, myofibroblasts proliferation, and ECM accumulation in the renal interstitium (Wang et al., 2016). According to our histopathological findings, the common pathological features of UUO were tubular injury and progressive interstitial fibrosis. On the other hand, biochemical findings of renal function exhibited an increase in Scr, BUN and microalbuminuria levels in the UUO-animals as compared to Sham-operated animals, however this increase was significant only at UUO 14- days group. Our observations were similar to other previous studies (Zhang et al., 2018).

TGF- β 1 is an inflammatory cytokine and considered the master regulator to drive fibrosis in all organs (Meng et al., 2016). One of the most characteristic finding of the present study was the increased TGF- β 1 mRNA expression after UUO in the obstructed kidney in comparison to the Sham-operated kidney. This increase in TGF- β 1 mRNA expression was more evident at UUO-14 days than UUO-7 days which also was more significant than UUO-3 days suggesting a gradual increase in TGF- β 1 mRNA expression among the different groups of UUO model. These findings were consistent with Lan Aiping, et al (Lan et al., 2014) who reported that the level of TGF- β 1 protein was increased in obstructed kidneys suggesting that amplified TGF- β 1 signaling was present in kidneys, which would have consequences for epithelial cells integrity in the renal tubules. This pattern of TGF- β 1 expression indicated that activation of TGF- β 1 signaling is a very early event occurs in renal fibrosis. Such TGF- β 1 is produced by infiltrating Inflammatory cells, parenchymal cells, and platelets during tissue repair (Jiang et al., 2014). It contributes to trans-differentiation of renal cells to myofibroblasts, leading to the production of ECM proteins (Meng et al., 2016).

In addition, TGF- β 1 is a potent inducer of EMT which has been suggested to be an important factor in the development of renal fibrosis (Johansson et al., 2015). One of the hallmarks of EMT is the de novo expression of vimentin in renal tubular epithelial cells. Vimentin is a member of the intermediate filament family of proteins. These proteins polymerize to form the basis of the cytoskeleton in fibroblasts (Wang et al., 2018). Our immunoblotting data showed that there was over expression of vimentin in in the obstructed kidney in comparison to the Sham-operated kidney. In accordance with other studies (Yuan et al., 2015), we found a significant evidence that the abnormal expression of Vimentin in the early stage (3 days) is indicative of the increase of interstitial cells, whereas in the later stage (14 days), EMT in tubules and the formation of irreversible interstitial fibrosis is suggested, therefore, Vimentin may be a potential marker for renal fibrosis.

In spite of the fact that TGF- β 1 stimulates several pathways, multiple studies have identified TGF- β 1/ Smad signaling as the main pathway in renal fibrosis (Meng et al., 2016). Among TGF- β 1/Smad signaling pathway, Smad3 plays a central role in renal inflammation and fibrosis. In order to assess its role in the development and progression of renal fibrosis, the current study aimed to investigate the expression pattern of Smad3 in mice with UUO in comparison to Sham-operated mice as controls. Results of the current study have established that there was over-expression of Smad3 protein in all groups of UUO model in comparison to the Sham-operated group with gradual increase from 3 days ligated group to reach its maximum in 14 days ligated group. Similar findings were also reported in other investigations (Yeh et al., 2010; Qin et al., 2011).

They found that TGF- β 1 treatment induced a significant increase in Smad3 which is required for the action of TGF- β signaling. These observations demonstrated the central role of Smad3 in the TGF- β 1/Smad signaling mediated renal fibrosis. Moreover, many fibrogenic genes e.g. collagens and EMT markers e.g. vimentin are Smad3-dependent and Smad3, directly binds to their DNA sequences to modulate expression of these target gene.

Although Smad4 has been known as a common Smad in the signal transduction pathway of the TGF- β family, its functional role and mechanism in TGF- β regulated inflammatory and fibrosis responses remain largely unclear, so another aspect of the current study was to investigate the impact of Smad4 in the regulation of TGF- β 1/Smad signaling pathway in renal fibrosis, via assessment of the expression pattern of Smad4, an important member of smad signals. Our findings revealed that there was an apparent over-expression of smad4 in fibrotic kidney tissues with UUO, especially 7 days and 14 days ligated groups, in comparison to the Sham-operated group. This finding was in agreement with Soji Kotaro, et al (Soji et al., 2018) who reported that Smad4 protein expression level was markedly increased in UUO mice as compared with sham controls. Over-expression of smad4 was accompanied by upregulation of Smad3 in all groups of UUO model. This can be attributed to the fact that Smad4 promotes Smad3-mediated renal fibrosis whereas, Smad4 is a critical regulator for the nuclear shuttling of Smad3, regulating its activity to initiate transcription of its target genes' expression (Lan, 2011).

Finally, the present study examined the tissue levels of some oxidative stress markers to assess their role in pathogenesis of renal fibrosis and clarify their link with TGF- β 1/Smad signaling in renal fibrosis development and progression. Outcomes of our study revealed a significant increase in the tissue level of MDA, the lipid peroxidation product and NO, a free radical in obstructed kidneys when compared to the normal kidneys. On the other hand, the increases in lipid peroxidation and NO levels were accompanied by obvious decrease in the antioxidant pool as manifested by diminished GSH levels and SOD activity, suggesting an important role of Oxidative stress in the pathogenesis of renal injury.

Although some previous studies demonstrated the role of both ROS and TGF- β 1/Smad signaling in the development of fibrosis (Said et al., 2018), only few studies highlighted the relationship between ROS and TGF- β 1 in the pathogenesis of renal fibrosis. Regarding to our results, TGF- β 1 can regulate ROS activity, not only by inducing their production, but also by down-regulating the expression of antioxidant enzymes such as superoxide dismutase (SOD), and the level of reduced glutathione (GSH). One possible mechanism which can explain the way by which TGF- β 1 decreases GSH concentration involves regulated expression of the GSH catalytic subunit gamma-glutamyl cysteine synthetase (GLC) (Krstić et al., 2015). ROS, in turn, can induce TGF- β 1 gene expression and activate its signaling through oxidizing latency association protein (LAP) or activating MMPs which promotes LAP release (Jiang et al., 2014), suggesting an interesting cycle of TGF- β 1, and ROS interplay.

In summary, in research into the Smad signaling pathway, the current study improved our understanding of the molecular mechanisms of renal fibrosis and inflammation in chronic kidney diseases. We demonstrated that Smad3 is a downstream

key mediator of TGF- β 1/Smad signaling and plays a pathogenic role in both renal inflammation and fibrosis. On the other hand, Smad4 is the common Smad and plays a vital role in promoting Smad3-mediated renal fibrosis. Most importantly, studying the potential role of oxidative stress in inducing renal fibrosis directly, or through the TGF- β dependent pathway, is an emerging area of investigation that needs to be addressed. Elucidating the mechanism of renal fibrosis pathogenesis associated with TGF- β 1/Smad signaling and ROS will contribute to the identification of therapeutic strategies to alleviate the costs and health burden of this disease.

FINANCIAL DISCLOSURE

This research did not receive any specific grant from funding agencies in the public, commercial, or not-for-profit sectors.

DECLARATION OF INTEREST SECTION

The authors report no declarations of interest.

AUTHOR'S CONTRIBUTIONS

H.S. and M.A. conceived and designed the presented idea, H.S. and A. H. performed the experiments, M.M. and A.A. verified the analytical methods, M.M and M.A. supervised the findings of this work, all authors discussed the results and contributed to the final manuscript.

REFERENCES

- Bao Y.-W., Yuan Y., Chen J.-H. and Lin W.-Q. J. Z. r. (2018):** Kidney disease models: tools to identify mechanisms and potential therapeutic targets. *Zoological Research*; 39(2): 72.
- Boor P. and Floege J. (2012):** The renal (myo-) fibroblast: a heterogeneous group of cells. *Nephrology Dialysis Transplantation*; 27(8): 3027-3036.
- Budi E. H., Duan D. and Derynck R. J. T. i. c. b. (2017):** Transforming growth factor- β receptors and Smads: regulatory complexity and functional versatility. *Trends in Cell Biology*; 27(9): 658-672.
- Chen D.-Q., Chen H., Chen L., Vaziri N. D., Wang M., Li X.-R. and Zhao Y.-Y. J. N. D. T. (2017):** The link between phenotype and fatty acid metabolism in advanced chronic kidney disease. *Nephrology Dialysis Transplantation*; 32(7): 1154-1166.
- Chen L., Yang T., Lu D.-W., Zhao H., Feng Y.-L., Chen H., Chen D.-Q., Vaziri N. D., Zhao Y.-Y. J. B. and Pharmacotherapy (2018):** Central role of dysregulation of TGF- β /Smad in CKD progression and potential targets of its treatment. *Biomedicine & Pharmacotherapy*; 101: 670-681.

- Chevalier R. L., Forbes M. S. and Thornhill B. A. (2009):** Ureteral obstruction as a model of renal interstitial fibrosis and obstructive nephropathy. *Kidney international*; 75(11): 1145-1152.
- Di Carlo S. E. and Peduto L. J. T. J. o. c. i. (2018):** The perivascular origin of pathological fibroblasts. *The Journal of Clinical Investigation*; 128(1): 54-63.
- Duffield J. S. J. T. J. o. c. i. (2014):** Cellular and molecular mechanisms in kidney fibrosis. *The Journal of Clinical Investigation*; 124(6): 2299-2306.
- El-Arbagy A. R., Yassin Y. S. and Boshra B. N. J. M. M. J. (2016):** Study of prevalence of end-stage renal disease in Assiut governorate, upper Egypt. *Menoufia Medical Journal*; 29(2): 222.
- El Agha E., Kramann R., Schneider R. K., Li X., Seeger W., Humphreys B. D. and Bellusci S. J. C. s. c. (2017):** Mesenchymal stem cells in fibrotic disease. *Cell stem cell*; 21(2): 166-177.
- Ellman G. L. (1959):** Tissue sulfhydryl groups. *Archives of Biochemistry and Biophysics*; 82(1): 70-77.
- Gibson-Corley K. N., Olivier A. K. and Meyerholz D. K. J. V. p. (2013):** Principles for valid histopathologic scoring in research. *Veterinary Pathology*; 50(6): 1007-1015.
- Jiang F., Liu G.-S., Dusting G. J. and Chan E. C. J. R. b. (2014):** NADPH oxidase-dependent redox signaling in TGF- β -mediated fibrotic responses. *Redox Biology*; 2: 267-272.
- Johansson J., Tabor V., Wikell A., Jalkanen S. and Fuxe J. J. F. i. o. (2015):** TGF- β 1-induced epithelial-mesenchymal transition promotes monocyte/macrophage properties in breast cancer cells. *Frontiers in Oncology*; 5: 3.
- Kendrick J. and Chonchol M. (2011):** The role of phosphorus in the development and progression of vascular calcification. *American Journal of Kidney Diseases*; 58(5): 826-834.
- Krstić J., Trivanović D., Mojsilović S., Santibanez J. F. J. O. m. and longevity c. (2015):** Transforming growth factor-beta and oxidative stress interplay: implications in tumorigenesis and cancer progression. *Oxidative Medicine and Cellular Longevity*; 2015: 654594.
- Lan A., Zhang J., Xiao Z., Peng X., Qi Y. and Du J. J. P. O. (2014):** Akt2 is involved in loss of epithelial cells and renal fibrosis following unilateral ureteral obstruction. *PLoS ONE*; 9(8): e105451.

- Lan H. Y. J. I. j. o. b. s. (2011):** Diverse roles of TGF- β /Smads in renal fibrosis and inflammation. *International Journal of Biological Sciences*; 7(7): 1056.
- Lee S.-Y., Kim S. I. and Choi M. E. J. T. R. (2015):** Therapeutic targets for treating fibrotic kidney diseases. *Translational Research*; 165(4): 512-530.
- Liu Y. (2010):** New insights into epithelial-mesenchymal transition in kidney fibrosis. *Journal of the American Society of Nephrology*; 21(2): 212-222.
- Lucarelli P., Schilling M., Kreutz C., Vlasov A., Boehm M. E., Iwamoto N., Steiert B., Lattermann S., Wäsch M. and Stepath M. J. C. s. (2018):** Resolving the combinatorial complexity of smad protein complex formation and its link to gene expression. *Cell Systems*; 6(1): 75-89.
- Lv J.-C. and Zhang L.-X. (2019):** Prevalence and Disease Burden of Chronic Kidney Disease. *Renal Fibrosis: Mechanisms and Therapies. Springer*; 3-15.
- Lv W., Booz G. W., Fan F., Wang Y. and Roman R. J. J. F. i. p. (2018):** Oxidative stress and renal fibrosis: recent insights for the development of novel therapeutic strategies. *Frontiers in Physiology*; 9: 105.
- Macias M. J., Martin-Malpartida P. and Massagué J. J. T. i. b. s. (2015):** Structural determinants of Smad function in TGF- β signaling. *Trends in Biochemical Sciences*; 40(6): 296-308.
- Marquez-Exposito L., Lavoz C., Rodrigues-Diez R. R., Rayego-Mateos S., Orejudo M., Cantero-Navarro E., Ortiz A., Egido J., Selgas R. and Mezzano S. J. F. i. p. (2018):** Gremlin regulates tubular epithelial to mesenchymal transition via VEGFR2: Potential role in renal fibrosis. *Frontiers in Pharmacology*; 9: 1195.
- Mathupala S. P., Heese C. and Pedersen P. L. (1997):** Glucose catabolism in cancer cells. The type II hexokinase promoter contains functionally active response elements for the tumor suppressor p53. *Journal of Biological Chemistry*; 272(36): 22776-22780.
- Meng X.-m., Nikolic-Paterson D. J. and Lan H. Y. J. N. R. N. (2016):** TGF- β : the master regulator of fibrosis. *Nature Reviews Nephrology*; 12(6): 325.
- Meng X.-M., Tang P. M.-K., Li J. and Lan H. Y. (2015):** TGF- β /Smad signaling in renal fibrosis. *Frontiers in physiology*; 6: 82.
- Mihara M. and Uchiyama M. (1978):** Determination of malonaldehyde precursor in tissues by thiobarbituric acid test. *Analytical Biochemistry*; 86(1): 271-278.

- Qin W., Chung A. C., Huang X. R., Meng X.-M., Hui D. S., Yu C.-M., Sung J. J. and Lan H. Y. J. J. o. t. A. S. o. N. (2011):** TGF- β /Smad3 signaling promotes renal fibrosis by inhibiting miR-29. *Journal of the American Society of Nephrology*; 22(8): 1462-1474.
- Said M. M., Azab S. S., Saeed N. M. and El-Demerdash E. J. A. o. h. (2018):** Antifibrotic mechanism of pinocembrin: impact on oxidative stress, inflammation and TGF- β /Smad inhibition in rats. *Annals of Hepatology*; 17(2): 307-317.
- Sessa W. C., Pritchard K., Seyedi N., Wang J. and Hintze T. H. J. C. r. (1994):** Chronic exercise in dogs increases coronary vascular nitric oxide production and endothelial cell nitric oxide synthase gene expression. *Circulation Research*; 74(2): 349-353.
- Soji K., Doi S., Nakashima A., Sasaki K., Doi T. and Masaki T. J. P. o. (2018):** Deubiquitinase inhibitor PR-619 reduces Smad4 expression and suppresses renal fibrosis in mice with unilateral ureteral obstruction. *PLoS One*; 13(8): e0202409.
- Suvarna K. S., Layton C. and Bancroft J. D. (2018):** Bancroft's Theory and Practice of Histological Techniques E-Book. *Elsevier Health Sciences*.
- Wang L., Ma J., Guo C., Chen C., Yin Z., Zhang X. and Chen X. J. B. r. i. (2016):** Danggui buxue tang attenuates tubulointerstitial fibrosis via suppressing NLRP3 inflammasome in a rat model of unilateral ureteral obstruction. *BioMed Research International*; 2016: 9368483.
- Wang S., Abouzied M. and Smith D. J. J. o. f. s. (1996):** Proteins as potential endpoint temperature indicators for ground beef patties. *Journal of Food Science*; 61(1): 5-7.
- Wang Z., Divanyan A., Jourdeuil F. L., Goldman R. D., Ridge K. M., Jourdeuil D. and Lopez-Soler R. I. J. A. J. o. P.-R. P. (2018):** Vimentin expression is required for the development of EMT-related renal fibrosis following unilateral ureteral obstruction in mice. *American Journal of Physiology-Renal Physiology*; 315(4): 769-780.
- Yeh Y.-C., Wei W.-C., Wang Y.-K., Lin S.-C., Sung J.-M. and Tang M.-J. J. T. A. j. o. p. (2010):** Transforming growth factor- β 1 induces Smad3-dependent β 1 integrin gene expression in epithelial-to-mesenchymal transition during chronic tubulointerstitial fibrosis. *The American Journal of Pathology*; 177(4): 1743-1754.
- Yuan Y., Zhang F., Wu J., Shao C. and Gao Y. J. S. r. (2015):** Urinary candidate biomarker discovery in a rat unilateral ureteral obstruction model. *Scientific Reports*; 5: 9314.

Zhang Z.-H., He J.-Q., Qin W.-W., Zhao Y.-Y. and Tan N.-H. J. C.-b. i. (2018): Biomarkers of obstructive nephropathy using a metabolomics approach in rat. *Chemico-Biological Interactions*; 296: 229-239.

Zhang Z.-H., Mao J.-R., Chen H., Su W., Zhang Y., Zhang L., Chen D.-Q., Zhao Y.-Y. and Vaziri N. D. J. C. b. (2017): Removal of uremic retention products by hemodialysis is coupled with indiscriminate loss of vital metabolites. *Clinical Biochemistry*; 50(18): 1078-1086.

تأثير إشارة عامل النمو المحول بيتا ١ / العائلة البروتينية سماد والإجهاد التأكسدي في مرض التليف الكروي. هل هناك رابط بينهما؟

*حمادة صبرى قبيصى ،^١ محمد أنور عبدالعزيز ،^١ أحمد على عبد الغنى ،^٢ مديحة محروس زخارى ،^٣ عبد الرازق هاشم عبد الرازق

^١ قسم الكيمياء الحيوية - كلية الصيدلة - جامعة الأزهر - أسيوط

^٢ قسم الكيمياء الحيوية - كلية الطب - جامعة أسيوط

^٣ قسم الأنسجة - كلية الطب البيطرى - جامعة بنى سويف

*البريد الإلكتروني للباحث الرئيسي : hamadaabozaid@azhar.edu.eg

المخلص :

يعتبر مرض الكلى المزمن واحدا من أكثر الأمراض انتشارا والمسببة للوفاة فى جميع أنحاء العالم. بغض النظر عن السبب الأولى ، فإن التليف الكروي هو المسار النهائي الشائع لجميع أمراض الكلى التي تؤدي بدورها إلى فشل الكلى المزمن . على الرغم من أن العديد من الدراسات القت الضوء على الدور المحتمل لكل من إشارة عامل النمو المحول بيتا ١ / العائلة البروتينية سماد والإجهاد التأكسدي في مرض التليف الكروي إلا أن القليل من الدراسات قد بحثت في العلاقة المحتملة بينهما ، وبالتالي فإن الدراسة الحالية تهدف إلى استكشاف تأثير كل من إشارة عامل النمو المحول بيتا ١ / العائلة البروتينية سماد والإجهاد التأكسدي على التليف الكروي من ناحية وتوضيح العلاقة بينهما من ناحية أخرى وذلك من خلال استخدام نموذج فئران تجارب والتي تعاني من انسداد فى الحالب الايسر . وقد اشتملت هذه الدراسة على قياس كلا من مستوى البروتينات المسماة سماد ٣ ، و سماد ٤ ، و الفيمنتين وذلك باستخدام طريقة الفصل الكهربائى للبروتينات . بينما تم قياس نسبة الجين المسمى عامل النمو المحول بيتا ١ بواسطة استخدام الناسخ العكسى لتفاعل البلمرة المتسلسل . هذا وقد تم أيضا تعيين مستويات أنسجة الكلى لكل من ثنائى ألدهيد المألون ، وأكسيد النيتروجين بالإضافة إلى الجلوتاثيون المختزل وكذلك نشاط انزيم السوبر اكسيد ديسميوتاز عن طريق التحليل الطيفى . ولقد أظهرت نتائج الدراسة الحالية وجود وفرة فى مستوى البروتينات المسماة سماد ٣ ، و سماد ٤ ، و فيمنتين مع وجود ارتفاع فى التعبير الجينى عن الحمض النووى الريبوزى الرسول لجين عامل النمو المحول بيتا ١ . هذا من ناحية ومن ناحية أخرى فقد لوحظ أن الزيادة فى التعبير الجينى عن الحمض النووى الريبوزى الرسول لجين عامل النمو المحول بيتا ١ كان مصاحبا لإختلال فى التوازن بين عوامل الأكسدة ومضاداتها مما يدل على وجود رابط بين عامل النمو المحول بيتا ١ وهذا الإختلال الحادث فى التوازن بين عوامل الأكسدة ومضاداتها.

الكلمات المفتاحية : مرض الكلى المزمن ، التليف الكروي ، انسداد الحالب من جانب واحد ، TGF-β1 ، Smad3 ، Smad4 ، Vimentin ، أنواع الأكسجين التفاعلية